

Reducing the In-plane Effect of Infill on Steel Moment Frame

A. Keyvani Borujeni^{1,*} and T. Mahdi²

¹Ph.D. Student, Road, Housing & Urban Development Research Center, Marvi St., Nargol St., Next to Shahrak Farhangian, Sheikh Fazlollah Noori Exp., Tehran, IRAN, P.O. Box: 13145-1696

²Assistant Professor, Road, Housing & Urban Development Research Center, Marvi St., Nargol St., Next to Shahrak Farhangian, Sheikh Fazlollah Noori Exp., Tehran, IRAN, P.O. Box: 13145-1696

Abstract

In this paper, four large-scale one-story steel moment-resisting frame specimens have been tested. The first specimen is a one-story steel moment-resisting frame without masonry infill walls. The second is similar to the first but with infill wall having full physical contact to the frame. The other two are non-structural infill walls. The first non-structural infill wall has a complete decoupling from the frame, while the second has a full contact at the top of the wall and separated from the columns. The results of this paper have shown that life safety performance level for non-structural infill wall having a complete decoupling from the frame has satisfied the allowable story drift. This was not the case for infill wall having full physical contact to the frame or nonstructural infill walls separated from two sides.

Keywords: Infill wall, Steel moment frame, Masonry, Non-structural infill, In-plane behavior

1. Introduction

According to ACI530 (ACI530, 2011), Masonry walls are divided into two categories:

(1) URM walls: In this system, the walls are considered as load-bearing ones. Due to the failure of many URM buildings in recent earthquakes, confined masonry walls have been considered as suitable replacements to URM walls. In this latter system, the wall is constructed first, followed by RC tie-columns. RC tie-beam is constructed on the top of the wall. Dual action is provided by the wall and confining framed system.

(2) Infilled RC or steel frames: In this system, the frame is constructed first, followed by the masonry wall. In infilled frames, infill walls are not load-bearing ones.

The failure of infill walls may very well be a significant threat for human life both inside and outside of the building as they are usually the first elements to experience damage even under moderate seismic events.

In common practice, and because of the complexity of the infill effect, infill walls are treated as non-structural elements and their influence on the behavior of the

structure is not considered. However; and due to their brittle behavior, the infill walls can modify the behavior of the structure leading to undesirable failure modes (Murty and Jain, 2000; Kappos and Ellul, 2000; AL-Chaar *et al.*, 2002; Lee and Woo, 2002; Magenes and Pampanin, 2004; Dolsek and Fajfar, 2008; Elnashai and Di Sarno, 2008; Di Sarno *et al.*, 2013; Preti *et al.*, 2012; Nicola *et al.*, 2015).

The infill walls are usually the first elements to be damaged in seismic events. Furthermore, Villaverde (1997) has shown that the cost related to the failure of a non-structural component in a building may easily exceed the replacement cost of a building, which is due to the loss of inventory, loss of business, downtime, etc. In the last three decades, several research programs have focused on the development of strengthening techniques for existing URM infill walls (Akin *et al.*, 2009; Akguzel, 2003). However, very few preventive measures have been suggested to avoid brittle failure, premature disintegration, and partial or total out-of-plane collapse of masonry infill walls during earthquakes (Calvi and Bolognini, 2001; Tasligedik *et al.*, 2011; Mosavi and Rafezi, 2012; Kuang and Wang, 2014). On the other hand, no substantial research efforts have been done for the development of improved solutions for new construction of URM infill walls. Accordingly, it is believed that further investigations are required to prevent the collapse of infilled walls or at least to reduce the cost of their repairs after seismic events.

Received July 26, 2016; accepted February 13, 2017;
published online September 30, 2017
© KSSC and Springer 2017

*Corresponding author

Tel: +989124337285, Fax: +98-21-88259977
E-mail: A.keyvani@bhrc.ac.ir

2. In-plane Cyclic Tests

2.1. General overview and main objectives

According to (Paulay and Priestley, 1992), two design alternatives on infill walls can be used. The first is to isolate the masonry infill walls from the bounding frame and the second is to use infill walls without full separation from the frame. However, it should be noted that even where sufficient separation is provided at top and ends of a panel, the panel will still tend to stiffen the supporting beam considerably, concentrating frame potential plastic hinge regions in short hinge lengths at each end, or forcing migration of hinges into columns, with a breakdown of the weak-beam, strong-column concept. In the second design alternative, the masonry walls are designed as structural elements and the contribution of the infill panels to the strength and stiffness of the frame needs to be recognized. Although these two approaches have been given in the NZS4230, there are no specific guidelines that support their design process. Practically and as explained before, since the influence of infill walls on the behavior of the structure is not considered, the first approach needs to be selected and gaps with sufficient widths need to be provided between the infill wall and top beam and side columns.

In order to stabilize the infill wall, mechanical connectors need to be added to ensure that the wall supports out-of-plane loads. However, such connectors must not transmit in-plane loads. On the other hand, the existence of gaps between infill walls and frames would eliminate the “Arching Action” and thereby reduce the out-of-plane resistance of infill walls. Based on the work of (Dawe and Seah, 1989), the gaps between the upper beams and Infill walls drastically reduce the ultimate strength of the infilled frame.

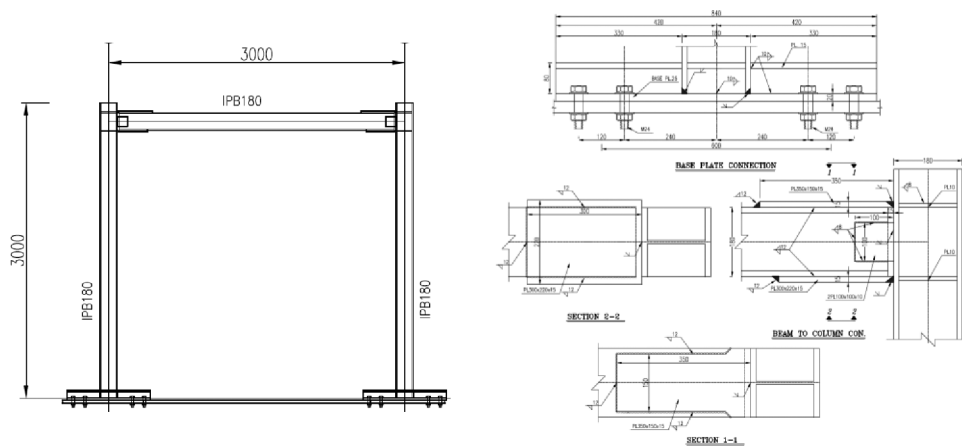
In this paper, four large-scale one-story steel moment-resisting frame specimens have been tested. Details of these frames are given in section 2-3.

2.2. Material characterization

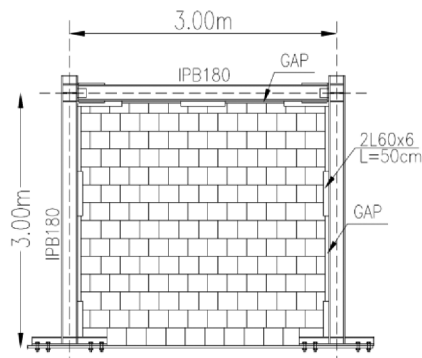
In this paper, lightweight horizontally perforated clay masonry units that are usually used for non-load bearing walls together with 1:4 cement-sand mortars were used to build the masonry infill walls. The steel was ST37.

2.3. Test setup description

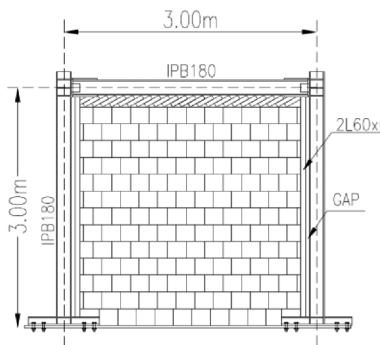
In the test program discussed here, four large-scale one-story steel moment-resisting frame specimens have been tested in the Structural Department Laboratory of Road, Housing, and Urban Development Research Centre



(a) Specimen F



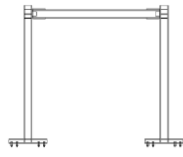
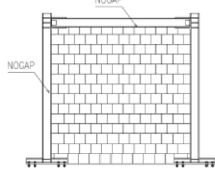
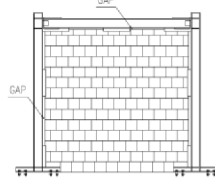
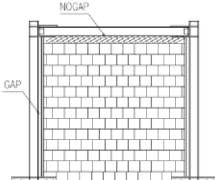
(b) Specimen N1



(c) Specimen N2

Figure 1. Two and three side separated detail.

Table 1. Specification of cyclic tests

Specimen name	Height	Span	Thickness	Gap (mm)		Structural Morphology
	H (cm)	L (cm)	T (cm)	Beam	Column	
F	300	300	-	-	-	
I	300	300	15	0	0	
N1	300	300	15	15	15	
N2	300	300	15	0	40	

(BHRC), Tehran, Iran.

The bounding frame was designed according to Iranian Code of Practice with medium ductility. All the columns and beams were IPB180 and special details were provided for the beam-column connection and the column-foundation intersection regions, as shown in Fig. 1. Each specimen was subjected only to in-plane cyclic loads and no vertical loads other than its weight were applied. In many previous works, vertical loads were considered and reported to have considerable effects on the strength and the stiffness of infilled frames (Mehrabi *et al.*, 1996). However, such effects are quite sensitive to the amount of such loads. To be on the safe side and to understand the effects of lateral loads, the present test program eliminated the vertical loads.

The first specimens is a one-story steel moment-resisting frame without masonry infill walls (Specimen F) while the other three are with infill walls and are follows:

(1) Steel moment-resisting frame with masonry infill wall having full physical contact to the frame (Specimen I).

(2) Steel moment-resisting frame with masonry infill isolated from beam and columns, as shown in Fig. 1 (Specimen N1). Mechanical connectors are provided to resist out-of-plane loads.

(3) Steel moment-resisting frame with masonry infill

wall having full contact at the top of the wall but isolated from columns, as shown in Fig. 1 (Specimen N2). Mechanical connectors are provided to resist out-of-plane loads.

The specification of all tests is shown in Table 1.

2.4. Loading conditions

For the first two tests, the ATC-24 protocol was used. However, and in order to have general loading history capable to cover the full range of deformation that the structure would experience under a severe earthquake excitation, a new loading protocol was used for the third and fourth tests, as shown in Fig. 2. This loading protocol was obtained from combining the ATC-24 and FEMA461 protocols. Both protocols were used in the past to evaluate the seismic performance of structures subjected to cyclic loads. However, ATC-24 protocol is designed for steel structures, while FEMA461 protocol is more appropriate for building parts or components sensitive to deformation such as frame assemblies.

In the third and fourth tests; and because of the existence of a gap between the infill wall and the frame, loading was not exerted on infill wall at the early stages. Thus, using ATC-24 was a suitable choice for loading in these early stages. On the other hand; when contact between frame and infill wall had occurred, the FEMA461 protocol

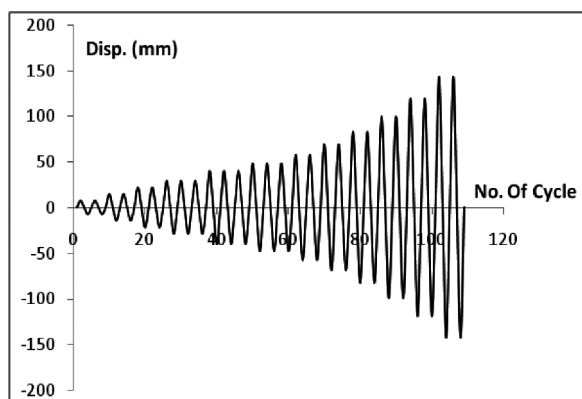


Figure 2. The loading protocol used for the third and fourth tests.

was more appropriate. In this new protocol, and in order to investigate the effect of repeated load on strength and stiffness degradation, two cycles each displacement amplitude were performed, as shown in Fig. 2.

3. Results of Tests

3.1. Steel moment frame without infill (Specimen F)

The load-displacement response of specimen F is given in Table 2. In this specimen, minor cracks were observed at one of the panel zones (beam-column intersection zones) during cycle 6 for a lateral load of 9.5 ton, and with an initial stiffness of 524 kg/mm and a drift of 0.6%, following the first noticeable decrease in lateral stiffness. Further decrease in lateral stiffness was observed at 0.8% drift as other cracks were observed near the base of one of the columns during cycle 8 for a lateral load of 11.5 ton, and with drift of 0.8%. Furthermore, the panel zone failed at drift=3% and the final failure occurred at the column base at the 4% drift with the final frame strength recorded

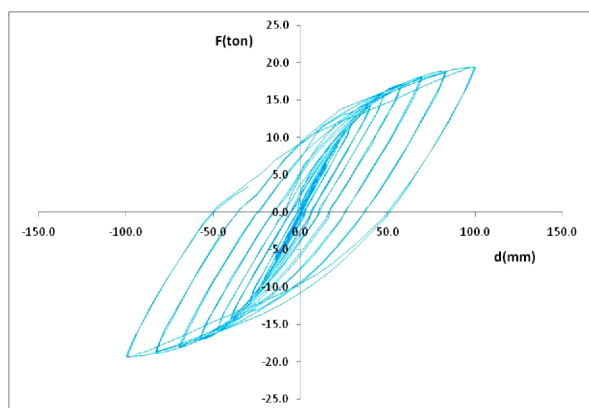


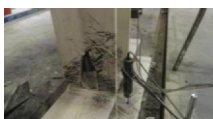
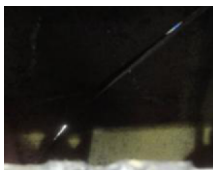

Figure 3. Hysteresis curve (Specimen F).

as 20.3 ton. Using the FEMA306 classification method, the performance levels of this specimen and the damage occurred in the infill wall at different drift levels are shown in Table 2. Furthermore, the hysteresis curve is shown in Fig. 3.

3.2. Infill wall with physical contact to the frame (Specimen I)

As shown in Table 3, the results of this test shows that infill increases the stiffness and strength of the composite frame. The first nonlinearity was observed at the 0.5% drift level combined with noticeable change of stiffness. At this early stage, some visible cracks between columns and walls were observed. For the following cycles and with increasing of the drift, the infill wall started developing cracks in the central part of masonry panel for drift between 0.2 and 0.5%. As a sequence of cracks' development, the shells of many blocks had fallen out. Then, diagonal cracks, stepped through joints, developed from the upper corner towards the centre of the walls. The damage had

Table 2. Performance level for bare frame (Specimen F)

	D (mm)	Drift	Description of damage
Insignificant (IO)	18.1	0.6%	
Moderate (LS)	90	3.0%	
Heavy (CO)	120	4.0%	

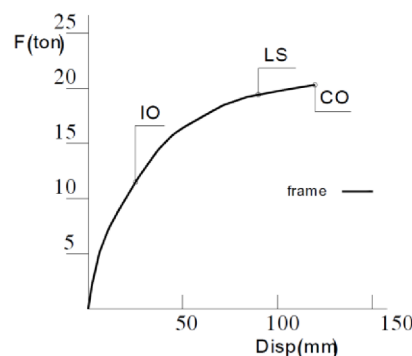



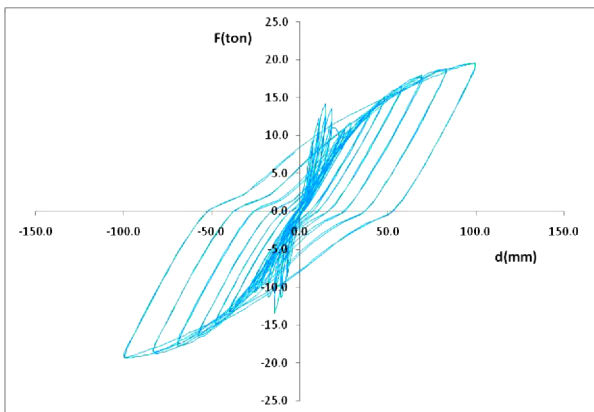
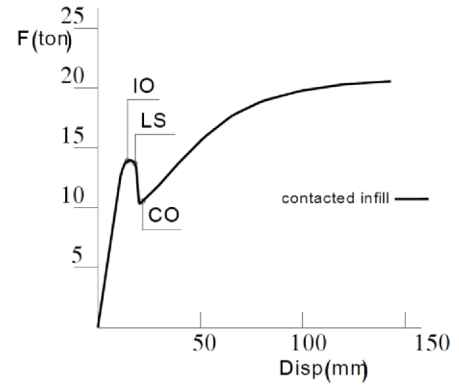


Table 3. Performance level for full contact infill frame (Specimen I)

	D (mm)	Drift	Description of damage
Insignificant (IO)	14.5	0.5%	
Moderate (LS)	18.1	0.6%	
Heavy (CO)	21.8	0.7%	

**Figure 4.** Hysteresis curve (Specimen I).

grown until the 0.7% drift level was achieved and as a sequence several block units were failed completely at the center of the infill wall. At this level, the infilled frame attained its maximum strength. It can be safely stated that from this drift level till the end of the test, lateral loads had been resisted only by the frame. This conclusion can also be reached from comparing the load-displacement curves, shown in Fig. 7.

Minor cracks were observed at one of the panel zones during cycle 16 for a lateral load of 14 ton and a drift level of 1.3%. Furthermore, cracks were observed near the base of one of the columns during cycle 23 for a lateral load of 17 ton, and with a drift of 2.3%. Finally, failures at the column base occurred at the 4.7% drift level with the final frame strength recorded as 20.6 ton.




Using the FEMA306 classification method, the

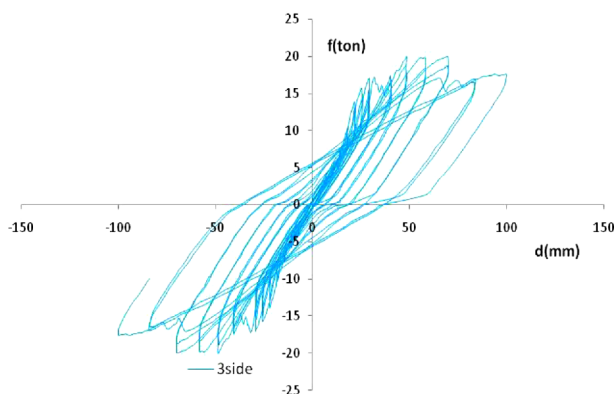
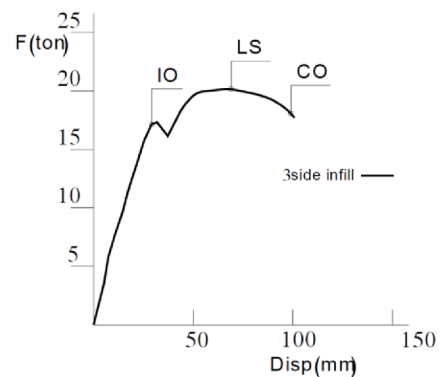
performance levels of this specimen and the damage occurred in the infill wall at different drift levels are shown in Table 3. In this test, collapse of block units at the center of the infill wall was the dominated type of failure. The hysteresis curve of this specimen is shown in Fig. 4. In this figure, the influence of the infill wall can be shown in the 0-15 mm displacement range. Furthermore, the initial stiffness of the infilled frame was obtained as 958 kg/mm. This stiffness is 1.8 times that assigned for the bare frame.

3.3. Nonstructural infill walls separated from three sides (Specimen N1)

In this test, the infill wall showed an initial stiffness a little higher than that of the bare frame. The first nonlinearity was observed at the 0.6% drift level combined with a noticeable change of stiffness. The first noticeable crack occurred at the corner of the wall and in the nearby of one of the steel angles. As shown in Table 4 and at cycle 13, the crack had 1200 mm length and 10 mm width. At this stage, a lateral load of 13 ton with an initial stiffness of 657 kg/mm and a drift level of 1.0% had been recorded. However, the main cracks were diagonal ones that developed in the central part of the wall and increased gradually in lengths and widths with the increase of the loads. The status of these cracks at cycle 23 for a 2.3% drift is shown in Table 4. It can be safely stated that from this drift level till the end of the test, lateral loads had been resisted only by the frame. This conclusion can also be reached from comparing the load-displacement curves, shown in Fig. 7. The specimen achieved its maximum strength of 20 ton at the 2% drift level. Furthermore, a

Table 4. Performance of the nonstructural infill frame (Specimen N1)

	D (mm)	Drift	Description of damage
Insignificant (IO)	29	1.0%	
Moderate (LS)	69.1	2.3%	
Heavy (CO)	99.5	3.3%	

**Figure 5.** Hysteresis curve (Specimen N1).

heavy failure of the infilled frame occurred at the 3.3% drift.

Minor cracks were also observed at one of the panel zones during cycle 7 for a lateral load of 11.9 ton and a drift level of 0.6%. However, none of these cracks were observed near the base of column.

From the current test, the initial stiffness of specimen N1 was around 657 kg/mm. This stiffness is 1.25 times that assigned for the bare frame. Thus, it can be concluded that using an infill wall with 15 mm separation joints had little effect on the initial stiffness of the infilled frame. Nevertheless, the frame strength increased. It is believed that the steel angles welded to the beam and columns had some role in such an increase.

Using the FEMA306 classification method, the performance levels of this specimen and the damage occurred in the infill wall at different drift levels are shown in Table 4.




The hysteresis curve of steel moment frame with three-side separated infill is shown in Fig. 5.

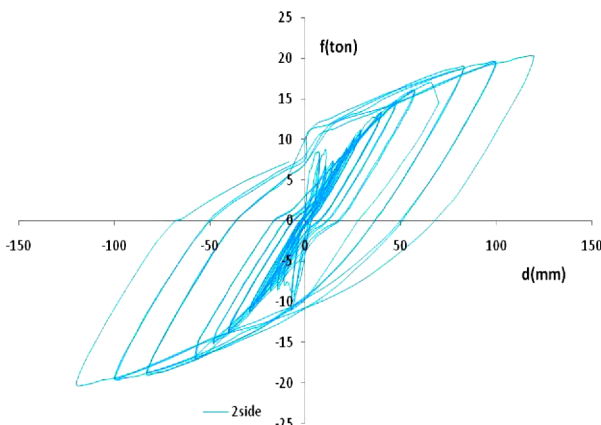
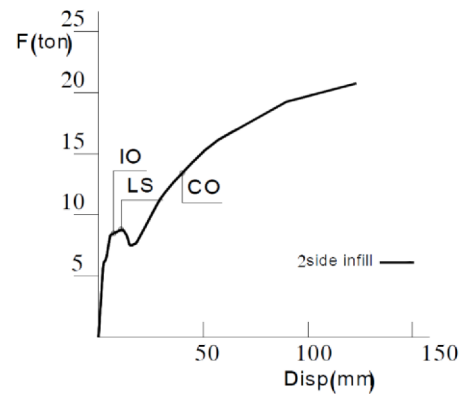
3.4. Nonstructural infill walls separated from two sides (Specimen N2)

In this test, the infill wall showed a considerable increase in its initial stiffness compared to that of the bare frame. The first nonlinearity was observed at the 0.1% drift level combined with noticeable change of stiffness. At this early stage, some visible cracks between Lshape and walls were observed. For the following cycles; and with increasing the drift, the infill wall developed cracks in the central part of masonry panel for drifts between 0.1 and 0.2%. At the end of cycle 2, minor cracks were observed at the center of wall for a lateral load of 8.5 ton, with an initial stiffness of 1164 kg/mm and drift level of 0.2%. The largest of these cracks had a width of 5 mm and a length of 800 mm. In later stages, stepped diagonal cracks formed through joints and extended toward the upper corners. This process continued until the 0.4% drift was reached. At this drift level, several cracks with different lengths were observed at the center of wall. The widths of these cracks ranged between 10 to 20 mm. During cycle 4, several block units completely failed. It can be safely stated that from this drift level till the end of the test, lateral loads had been resisted only by the frame. This conclusion can also be reached from comparing the load-displacement curves, shown in Fig. 7.

Minor cracks were observed at one of the panel zones during cycle 14 for a lateral load of 11 ton and a drift level of 0.9%. The cracks were observed at near the base of one of the columns during cycle 21 for a lateral load

Table 5. Performance level of nonstructural infill walls separated from two sides (Specimen N2)

	D (mm)	Drift	Description of damage
Insignificant (IO)	7.3	0.2%	
Moderate (LS)	10.9	0.4%	
Heavy (CO)	40	1.3%	

**Figure 6.** Hysteresis curve (Specimen N2).

equal to 16 ton, with drift equal to 1.9%. Finally, failures at base of one of the columns occurred at the 4.5% drift and the strength of the infilled frame reached the mark of 22 tons.

Using the FEMA306 classification method, the performance levels of this specimen and the damage occurred in the infill wall at different drift levels are shown in Table 5. In this test, collapse of block units was the dominated type of failure. The hysteresis curve of this specimen is shown in Fig. 6.

Although a 40 millimeter gap from the column had been used in this test, the initial stiffness of specimen N2 was around 1164 kg/mm. This stiffness is 2.2 times that assigned for the bare frame. Thus, the effect of the infill

wall on the frame initial stiffness was quite clear in this test. It is believed that the steel angles welded to the beam had some role in such behavior, since its effect diminished after the failure of the weld. After drift=0.4%, the welding of the L shape steel angles failed one after the other and the influence of the infill wall on the stiffness became less noticeable.

4. Discussion of Results

4.1. Separation details

Because the structural infill walls start cracking in low drift, its performance does not meet life safety level. Therefore, it seems that there is a need for further work to be done in order to have proper details and reliable models for the isolation of infill walls. This detail makes the infill as a non-structural one. Two cases are considered for non-structural walls, and they are as follows:

In first case (the gaps between the infill wall and top beam and side columns), welded Lshape changed the infill frame stiffness slightly. But, because of gap, the masonry infill does not change until drift 0.5%. Also, infill crack occurred in blocks interface and crack spreading is continued until life safety drift (2%). Therefore, the performance meet life safety level for non-structural members and this detail is suitable for separation. However, little improvement is needed.

In second case (the gaps between the infill wall and side columns), the vertical Lshape significantly increases the initial stiffness before weld failure at drift 0.4%. From Fig. 9, it can be seen that this case is in good agreement

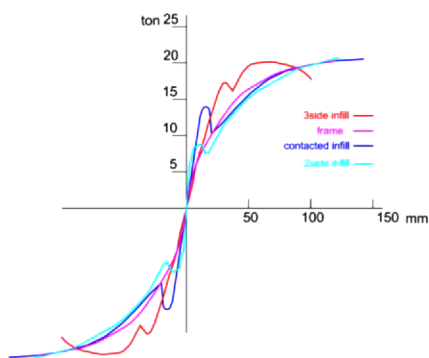


Figure 7. Infill frame load-displacement curve.

with bare frame after drift 0.4% to 1.3%. Because of the Lshape on the vertical edges, full separation is not created at the beginning of loading before drift 0.4%. However, the Infill cracking starts in drift 0.2% and extends until 0.4%. Therefore the infill wall failed in low drift. Therefore, the performance does not meet life safety level for non-structural members. It can be concluded that using the welding for the vertical Lshape is not suitable.

4.2. Effect of separation on infill participation

The results of specimen N1 show that infill increases the initial stiffness of the infilled frame lowly. However, infill of specimen N2 highly increases the initial stiffness. Due to improper details in Specimen N2, the infill walls participated as structural walls in the early stages of loadings.

4.3. Stiffness

The ideal three line curves can be drawn based on FEMA306. As shown in Table 6, the gaps between the infill wall and top beam and side columns in specimen N1 had changed the frame stiffness slightly. However, the gaps between the infill wall and side columns in specimen N2 had extensively changed the frame stiffness.

4.4. Performance level

According to Fig. 8 and Tables 2 to 5, life safety level was satisfied at drift 3.0, 0.7, 2.3, 0.4% for specimen F, I, N1, N2, respectively. Therefore, bare and nonstructural infill walls separated from three sides had satisfied life safety performance level. But full contacted infill wall and nonstructural infill walls separated from three sides had not satisfied this level.

4.5. Plastic hinge at the base of the frame

The strain-displacement curve is shown in Fig. 9. In the bare frame, the bottom of column had yielded at drift 0.8% and the strain continued until $5.5\epsilon_y$ (ϵ_y is yield strain). In specimen I, the yield occurred in drift 1.8%, since the infill wall prevented the yield of the columns before of this drift. The strain is continued until $5.5\epsilon_y$. This figure illustrat that the column in specimen N1 had not yielded until drift 3.3% because of the welded Lshape angle to columns, since it changed behavior of frame. In specimen N2, the yield occurred in drift 1.6%. In this case as well, the infill wall prevented the yield of columns before of this drift. The strain is continued until $5.5\epsilon_y$.

Table 6. Ideal curve parameters

	H_{cr} (ton)	d_{cr} (mm)	H_{max} (ton)	d_{Hmax} (mm)	H_{dmax} (ton)	d_{max} (mm)	K_e (Kg/mm)	K_{Hmax} (Kg/mm)
F	9.5	18.1	20.3	120	-	-	524	169
I	13.9	14.5	20.6	143	-	-	958	52
N1	11.9	18.1	17.7	64.2	20.1	101	657	126
N2	8.5	7.3	20.7	123	-	-	1164	168

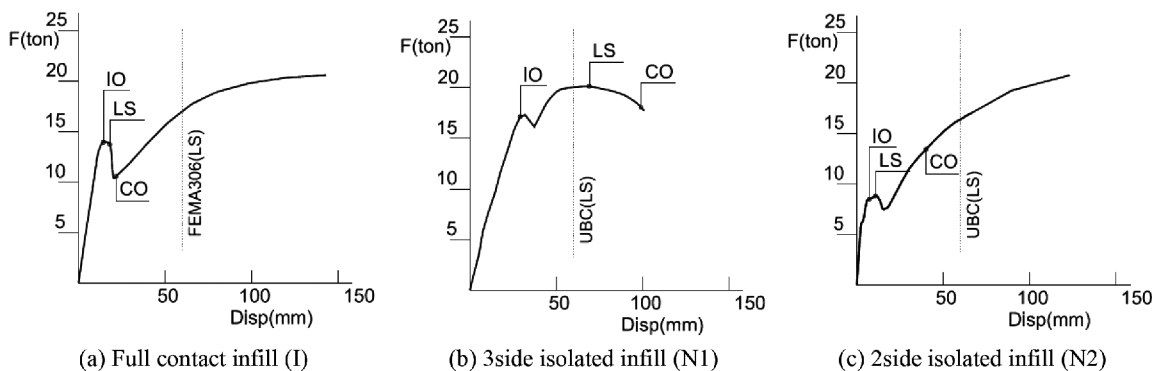


Figure 8. Performance level

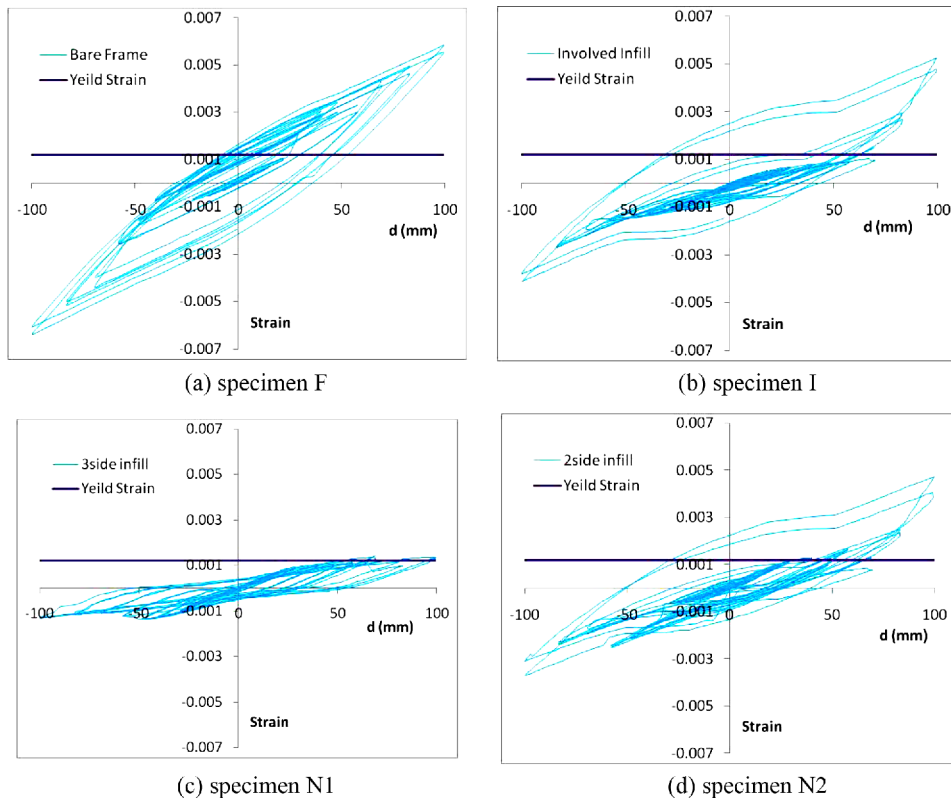


Figure 9. Strain hysteresis curve.

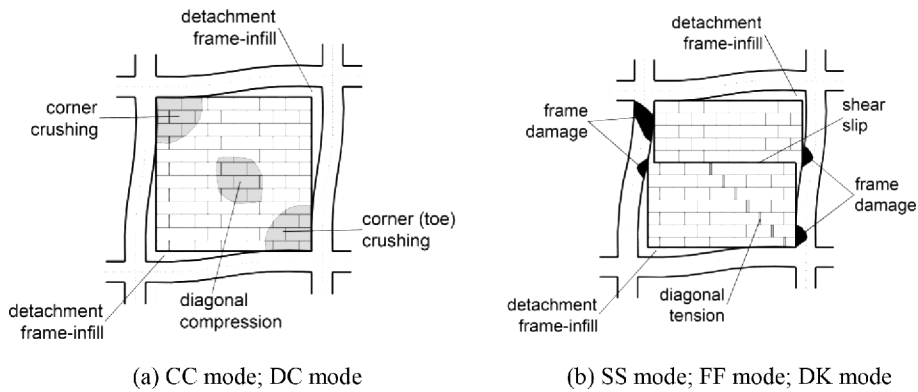


Figure 10. Modes of failure of masonry infill frames.

4.6. Failure Modes

Based on both experimental and analytical results during the last five decades (Thomas, 1953; Wood, 1958; Mainstone, 1962; Liauw and Kwan, 1983; Mehrabi and Shing, 1997; Al-Chaar *et al.*, 2002) different failure modes of masonry in-filled frames were observed, that can be classified into five distinct modes (Wood, 1978; El-Dakhakhni, 2002; Ghosh and Amde, 2002; El-Dakhakhni *et al.*, 2003) given below:

(1) The Corner Crushing (CC) mode, which represents crushing of the infill in at least one of its loaded corners, as shown in Fig. 10(a). This mode is usually associated with in-filled frames consisting of a weak masonry infill

panel surrounded by a frame with weak joints and strong members.

(2) The Diagonal Compression (DC) mode, which represents crushing of the infill within its central region, as shown in Fig. 10(a). This mode is associated with a relatively slender infill, where failure results from out-of-plane buckling of the infill.

(3) The Sliding Shear (SS) mode, which represents horizontal sliding shear failure through bed joints of a masonry infill, as shown in Fig. 10(b). This mode is associated with infill of weak mortar joints and a strong frame.

(4) The Diagonal Cracking (DK) mode, which is seen

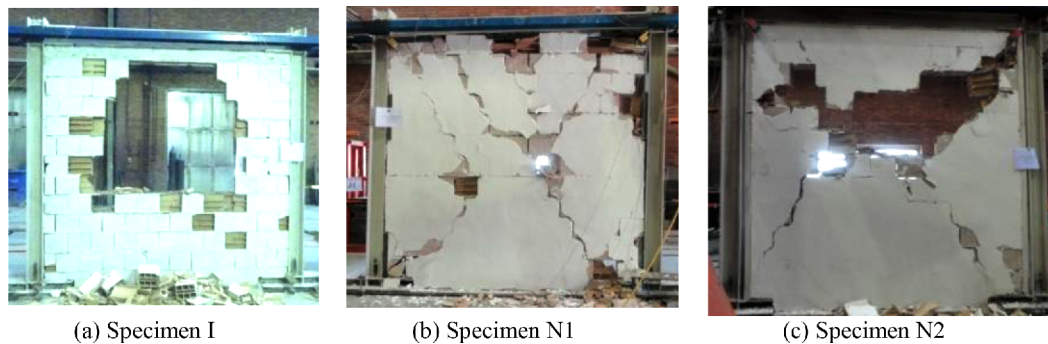


Figure 11. Modes of failure of infill.

in the form of a crack across the compressed diagonal of the infill panel and often takes place with simultaneous initiation of the SS mode, as shown in Fig. 10(b). This mode is associated with a weak frame or a frame with weak joints and strong members in-filled with a rather strong infill.

(5) The Frame Failure (FF) mode, which is seen in the form of plastic hinges developing in the columns or the beam-column connections, as shown in Fig. 10(b). This mode is associated with a weak frame or a frame with weak joints and strong members in-filled with a rather strong infill.

According to Fig. 11, specimen I and N2 have the diagonal compression failure mode. But specimen N1 have the diagonal tension failure mode.

5. Conclusions

Experimental studies have shown that structural infill walls have a major influence on behavior of structures. However, in seismic analysis and design, engineers typically ignore the additional stiffness and strength that the partitions may provide, which could prove to be beneficial or detrimental to the buildings. The purpose of this research is studying the effect of hollow block partitions on structural response of buildings. Thus, four steel frames in one story were tested and the effect of two types of wall separations (nonstructural infill wall separated from two and three sides) on seismic behavior of frame was investigated.

The results showed that for infill wall with physical contact to the frame, the initial stiffness and strength is increased considerably and therefore performance Level is different from those expected. Similar results had been found for nonstructural infill wall separated from two sides. Therefore, the effect of infill walls should be considered particularly for both life safety and collapse level. On other hand, the increase in initial stiffness and strength were less than those of nonstructural infill wall separated from three sides, and performance level was the same as those expected. Therefore, the effect of this non-structural partition can be ignored particularly for life safety and collapse levels.

Furthermore, no strength degradation was observed before 0.6, 0.4 and 2.3% drift for full contact, two sides separated and three sides separated infill, respectively.

For all specimens, the maximum strength was characterized by diagonal crack starting in the panel after 0.2% drift when the side column/strut in both panels became clearly detached.

On the basis of the results of the experimental work presented in this paper, the following conclusions may be drawn:

- (1) The influence of specimen I and N2 on the seismic response of the steel frame is significant. But influence of specimen N1 is negligible.
- (2) Masonry infill increases the initial elastic stiffness and the lateral maximum capacity of the steel frame in specimen I, N2 but not to specimen N1.
- (3) The main failure mode of specimen I, N2 was in the form of diagonal compression. But the failure mode of specimen N1 was diagonal tension.
- (4) In the specimen N1, welded Lshape angles changed the behavior of steel frame.
- (5) In specimen N2, and due to improper detail, the stiffness of the infilled frame was increased.
- (6) For the reference infill (specimen I), damage occurred at a lower drift level.
- (7) Based on the observed damage occurred in different specimen, separation of infill wall from the frame had resulted in better over-all behavior of the structure.

References

- ACI 530 (2011). "Building Code Requirements for Masonry Structures", Reported by the Masonry Standards Joint Committee
- AL-Chaar, G., ISSA, M. and Sweeney S. (2002). "Behavior of masonry-infilled no ductile reinforced concrete frames", *J. of Struct. Eng.*, 128(8), pp. 1055-1063.
- Akin, E., Ozcebe G., and Ersoy U. (2009). "Strengthening of Brick Infilled RC Frames with CFRP Sheets", *Seismic Risk Assessment and Retrofitting-Geotechnical, Geological, and Earthquake Engineering*. Vol 10, Ch 18, pp. 367-386.
- Akguzel, U. (2003). "Seismic Retrofit of Brick Infilled R/C Frames with Lap Splice Problems in Columns", MS

- Thesis, Department of Civil Engineering, Bogazici University, Istanbul, Turkey.
- Calvi, G. M. and Bolognini, D. (2001). "Seismic Response or Reinforced Concrete Frames Infilled with Weakly Reinforced Masonry Panels", *Journal of Earthquake Engineering*, 5(2), pp. 153-185.
- Dolsek, M. and Fajfar, P. (2008). "The Effect of Masonry Infills on the Seismic Response of a Four-Storey Reinforced Concrete Frame-A Deterministic Assessment", *Engineering Structures*, 30, pp. 1991-2001.
- Dawe, J. L. and Seah, C. K. (1989). "Out-of-plane resistance of concrete masonry infilled panels", *Can. J. Civ. Eng.*, 16, pp. 854-864.
- Di Sarno, L., Yenidogan, C., and Erdik, M. (2013). Field evidence and numerical investigation of the Mw=7.1 October 23 Van, Tabanlı and the Mw>5.7 November Earthquakes of 2011. *Bulletin of Earthquake Engineering*, 11(1), pp. 313-346
- Elnashai, A. S. and Di Sarno, L. (2008). "Fundamental of earthquake engineering", Wiley, West Sussex, UK.
- Kappos, A. J. and Ellul, F. (2000). "Seismic design and performance assessment of masonry-infilled R/C frames", *Proceedings of the 12th WCEE*, paper 989, New Zealand.
- Kuang, J. S. and Wang, Z. (2014). "Cyclic Load Tests of RC Frame With Column-Isolated Masonry Infills", *Second European Conference On Earthquake Engineering And Seismology*, Istanbul AUG, pp. 25-29.
- Lee, H. S. and Woo, S. W. (2002). "Effect of Masonry Infills on Seismic Performance of a 3-Storey R/C Frame with Non-Seismic Detailing", *Earthquake Engng Struct. Dyn.*, 31, pp. 353-378.
- Magenes, G. and Pampanin, S. (2004). "Seismic Response of Gravity-Load Design Frames with Masonry Infills", *13th World Conference on Earthquake Engineering*, August 1-6, 2004, Paper No. 4004, Vancouver, Canada.
- Mehrabi, A. B., Benson Shing, P., Schuller, M. P., and Noland, J. L. (1996). "Experimental evaluation of masonry-infilled RC frames. *Journal of Structural Engineering*, 122(3), pp. 228-237.
- Murty, C. V. R. and Jain, S. K. (2000). "Beneficial influence of masonry infill walls on seismic performance of RC frame buildings", *Proceedings of 12th WCEE*, paper 1790.
- Mosavi, M. and Rafezi, B. (2012). "Effect of separation of masonry infill from peripheral concrete frame on seismic behavior of composite frame", NCCAF.
- Nicola, T., Leandro, C., Guido, C., and Enrico, S. (2015). "Masonry Infilled Frame Structures: State-Of-The-Art Review Of Numerical Modelling", *Earthquakes and Structures*, 8(3), pp. 731-757
- Paulay, T. and Priestley, M. J. N. (1992). "Seismic Design of Reinforced Concrete and Masonry Buildings", Christchurch, San Diego, John Wiley and Sons. pp. 584-595.
- Preti, M. M., Bettini, N. N., and Plizzari, G. G. (2012). "Infill walls with sliding joints to limit infill-frame seismic interaction: Large-scale experimental test", *Journal of Earthquake Engineering*, 16(1), pp. 125-141
- Tasligedik, A. S., Pampanin, S., and Palermo, A. (2011). "Damage Mitigation Strategies of 'Non-Structural' Infill Walls: Concept and Numerical-Experimental Validation Program", *Proceedings of the Ninth Pacific Conference on Earthquake Engineering, Building an Earthquake-Resilient Society*, 14-16 April, 2011, Auckland, New Zealand.
- Villaverde, R. (1997). "Seismic Design of Secondary Structures: State of the Art." *ASCE Journal of Structural Engineering*, 123(8), pp. 1011-1019.